



Real-Time Experimental Assessment of Hill Climbing MPPT Algorithm Enhanced by Estimating a Duty Cycle for PV System

Claude Bertin Nzoundja Fapi, Patrice Wira, Martin Kamta, Abderrezak Badji, Hyacinthe Tchakounté

► To cite this version:

Claude Bertin Nzoundja Fapi, Patrice Wira, Martin Kamta, Abderrezak Badji, Hyacinthe Tchakounté. Real-Time Experimental Assessment of Hill Climbing MPPT Algorithm Enhanced by Estimating a Duty Cycle for PV System. International Journal of Renewable Energy Research, 2019, 9 (3), pp.1180-1189. hal-03265246

HAL Id: hal-03265246

<https://hal.science/hal-03265246>

Submitted on 19 Jun 2021

HAL is a multi-disciplinary open access archive for the deposit and dissemination of scientific research documents, whether they are published or not. The documents may come from teaching and research institutions in France or abroad, or from public or private research centers.

L'archive ouverte pluridisciplinaire **HAL**, est destinée au dépôt et à la diffusion de documents scientifiques de niveau recherche, publiés ou non, émanant des établissements d'enseignement et de recherche français ou étrangers, des laboratoires publics ou privés.

Real-Time Experimental Assessment of Hill Climbing MPPT Algorithm Enhanced by Estimating a Duty Cycle for PV System

Claude Bertin Nzoundja Fapi^{*,**‡}, Patrice Wira^{**}, Martin Kamta^{*}, Abderrezak Badji^{**,***}, Hyacinthe Tchakounte^{*}

^{*}LESIA Laboratory, University of Ngaoundere, P. O. Box: 455 Ngaoundere, Cameroon

^{**}IRIMAS Laboratory, Haute Alsace University, 61 Rue Albert Camus, 68200 Mulhouse, France

^{***}LATAGE Laboratory, Mouloud Mammeri University of Tizi-Ouzou, BP: 17 RP 15000 Tizi-Ouzou, Algeria

(nzoufaclauber@yahoo.fr, patrice.wira@uha.fr, martin_kamta@yahoo.fr, badji_ummto@yahoo.com, tchakounte_hyacinthe@yahoo.fr)

[‡]Corresponding Author: Claude Bertin Nzoundja Fapi, 50 Boulevard Charles Stoessel, 68200 Mulhouse, France,
Tel: +33 75 24 24 254, nzoufaclauber@yahoo.fr

Received: 18.04.2019 Accepted: 08.06.2019

Abstract- Better functioning of maximum power point tracking (MPPT) can significantly increase the energy efficiency of photovoltaic systems. This process is provided by MPPT algorithms. Such as fractional open-circuit voltage, perturb and observe, fractional short-circuit current, hill climbing, incremental conductance, fuzzy logic controller, neural network controller, just to name a few. The hill climbing algorithm uses the duty cycle of the boost converter as a retraction parameter when the MPPT task is performed. However, this technique has disadvantages in terms of the stability of the system during periods of constant radiation. To overcome this disadvantage, A MPPT technique based on the estimation of the boost converter duty cycle associated with the conventional hill climbing, fractional open-circuit voltage and fractional short-circuit current algorithm is proposed. A comprehensive description of the experimental implementation hardware and software platforms is presented. On the basis of the measured data, the enhanced algorithm was compared to the conventional hill climbing MPPT technique according to various criteria, showing the disadvantages and advantages of each. Experimental results show advantage of the enhanced algorithm compared to the conventional hill climbing MPPT technique in time response attenuation (0.25 s versus 0.6 s), little oscillations (0.5 W versus 2.5 W), power loss reductions and better maximum power point tracking accuracy (98.45 W versus 92.75 W) of the enhanced algorithm compared to the conventional hill climbing MPPT technique.

Keywords: Hill Climbing algorithm, maximum power point tracking (MPPT), experimental result, photovoltaic.

1. Introduction

In recent years, the demand for electrical energy never stopped while at the same time the constraints related to its production increased [1], [2]. Indeed, more and more power will be produced by the photovoltaic (PV) process which converts sunlight into electricity. The drawbacks of this source of energy are the intermittence of the PV source and the fact that power supplied by the PV generator depends on unpredictable weather conditions. In order to overcome

them, the maximum power point tracking (MPPT) technics can be applied. Furthermore, the MPPT is a reliable method to extract at any time the maximum power in order to optimize the energy production. Indeed, the improvement of the photovoltaic generator requires optimal operation of the DC-DC converters used as an interface between the PV generator and the load to be supplied [3]-[5].

A wide range of MPPT algorithms have been developed to ensure optimal operation of the photovoltaic system. We can mention traditional MPPT methods which mainly

include the following perturb and observe (P&O) [6], [7], fractional open-circuit voltage (FOCV) [8], [9], fractional short-circuit current (FSCC) [8], [9], incremental conductance, hill climbing (HC) [10], [11], while the intelligent MPPT control method includes the neural network, fuzzy logic control (FLC) [3]-[6], [10], [12]-[15], genetic algorithms, particle swarm optimization, teaching-learning-based optimization [3]-[6]. Among all the previous MPPT strategies, in [9] the authors compare performances and tracking accuracy between the bisection numerical algorithms based MPPT with the FSCC and FOCV MPPT methods. A new digital control scheme for a standalone PV system using fuzzy logic and a dual MPPT controller is presented in [14]. A new FLC for MPPT of PV systems is proposed in [12]; the author uses the hill climbing search method by fuzzifying the rules of such techniques and suppresses their drawbacks. In [16], the conventional P&O method, various weather conditions by using the FSCC algorithm is proposed. An hybrid version of P&O algorithm, short-circuit current and open-circuit voltage techniques with improved relations are derived in [17]. To minimize insufficiency effect of the classic incremental conductance method, the proposed method in [18] developed a new incremental conductance controller based on a fuzzy duty cycle change estimator with direct control.

Various MPPT algorithms have adopted the hybrid approach to improve the efficiency of MPPT [8], [9], [11], [18]-[20]. In Ref. [14], the method samples short-circuit current (I_{sc}) and open-circuit voltage (V_{oc}) are used to locate maximum power point (MPP). However, the information regarding the procedure of the short-circuit current and open-circuit voltage is missing. The methods presented in Refs. [9], [16] are based on the association of P&O and FOCV MPPT algorithms. Techniques in [20] measure the open-circuit voltage to estimate the maximum voltage but lack a separate strategy for the estimation of duty cycle of the boost

converter. Considering these disadvantages, this paper presents a new enhanced MPPT method, which is the association of hill climbing, fractional open-circuit voltage and fractional short-circuit current algorithms. The main aim is to try to improve hill climbing method by combining fractional open-circuit voltage and fractional short-circuit current, while keeping the control technique simple. The particularity of the enhanced MPPT resides in the fact that, the relations are developed to estimate the maximum voltage and the maximum current without open-circuiting and short-circuiting of the PV array. Using the maximum current and the maximum voltage magnitudes, a new duty cycle optimization method expression is designed for the DC-DC boost converter. This suppresses the need of any control schemes (PI/PID etc...).

To validate the proposed method, much performance should be evaluated like: the number of variables (number and type of sensors used), the control strategy (indirect control, direct control or probabilistic control), the tracking style (analogic or digital implementation) and the result of tracking (Accuracy and speed of tracking) [3, 5, 10, 21]. The proposed MPPT is ideally suited for standalone and DC-load PV systems. To check the validity of the proposed algorithms several tests with real-time weather conditions have been carried out. The electrical synoptic of experimental configuration of the PV system is illustrated in Fig. 1. In this figure, the acquisition unit must acquire measured analog signals (current and voltage of the PV panel). These signals are processed by the DS1104 control board and sent by means of Slave I/O pulse width modulation (PWM) channels to the PWM controller to drive the DC-DC boost converter.

The enhanced hill climbing MPPT algorithm and proposed method are presented in Section II. Section III presents the experimental test implementation and results. Section IV concludes the work.

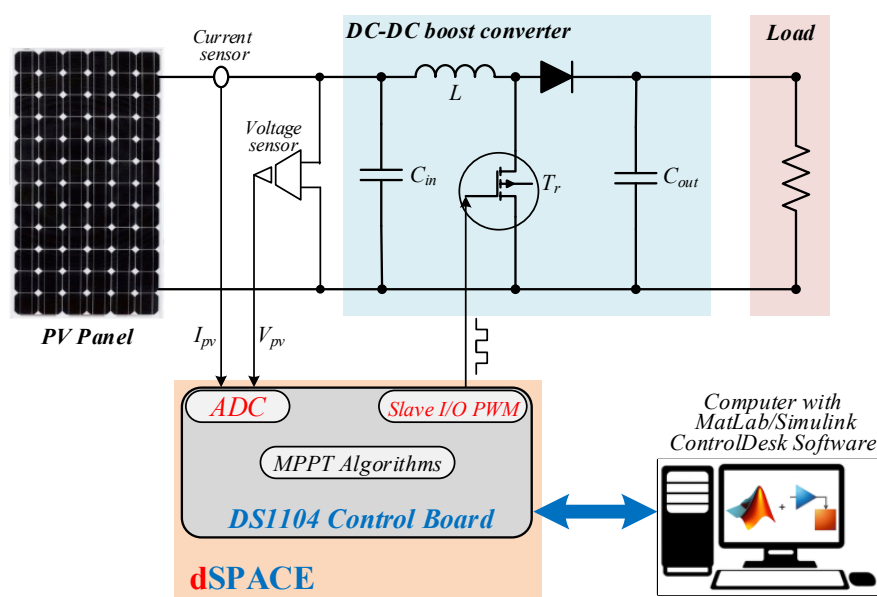


Fig. 1. Electrical synoptic scheme of experimental setup of the PV system.

2. Enhanced MPPT algorithm for PV systems

To enhance the output power of PV panels, the MPPT algorithms used gradually decrease or increase the duty cycle of the converter used as the interface between the load and the PV panel.

2.1. The fractional open-circuit voltage (FOCV) and fractional short-circuit current (FSCC) method

The FOCV method consists in comparing the voltage delivered by the PV panel with the maximum voltage (V_{mpp}) considered as a reference [1], [4]. The reference voltage is obtained from the linear relationship between V_{mpp} and V_{oc} of the PV module [5], [9]:

$$V_{mpp} = K_v \times V_{oc} \quad (1)$$

where K_v is the voltage proportionality constant.

The disadvantage of this technique is that it is necessary to perform the V_{oc} measurement from time to time. The load must therefore be disconnected during this measurement, resulting in a loss of power.

The FSCC algorithm is one of the simplest offline techniques. The MPPT obtained using this technique is calculated using Eq. (2) [5], [8].

$$I_{mpp} = K_i \times I_{sc} \quad (2)$$

where K_i is the current proportionality constant.

Despite the fact that the implementation of this method is simple and inexpensive, its performance is comparatively low due to the utilization of inexact values of K_i in the computation of I_{mpp} . FSCC MPPT requires only a current sensor and is consequently less costly. The disadvantage is the recurring loss of power when the short-circuit current is measured [1], [8].

2.2. Hill climbing algorithm

The best thing about the hill climbing MPPT method is its simplicity (see Fig. 2). It uses the duty cycle of the boost converter as feedback parameter when the task of the MPPT is carried out [10], [12]. The main disadvantage of this technique is due to the trade-off between the stability of the system in a period of constant irradiation. Another disadvantage is the absence of a rapid response in case of a rapid change in radiation [10], [12]. The period of steady radiation requires a very small value of variation in the duty cycle, ΔD to avoid a strong oscillation of the power about the peak power point, reducing the energy captured by the PV. On the other hand, rapidly changing irradiation requires a higher duty cycle value to accelerate the pursuit of peak power.

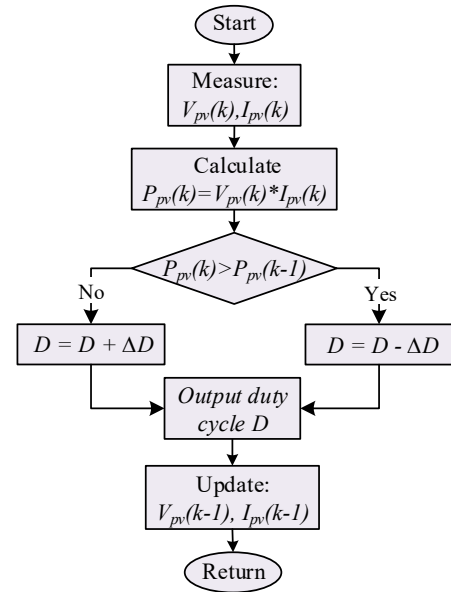


Fig. 2. State flowchart of hill climbing MPPT technique.

2.3. The Proposed MPPT Method

There are several factors to consider when developing and choosing MPPT execution techniques, such as costs, convergence speed, and the ability of an algorithm to detect several maxima quickly. The enhanced technique is developed to improve the efficiency of conventional hill climbing by reducing the oscillation to the steady state and preventing its divergence at the maximum power point locus. As with other types of hill climbing technique, the enhanced method is based on the P-V characteristic curve of the photovoltaic grid and the MPP is followed by evaluating the differential sign of power calculated by the estimated values of V_{mpp} and I_{mpp} as a function of voltage. When the D_{mpp} estimates in operation reaches the neighborhood of the maximum power point, the size of the disturbance step is diminished to a minimum value by the variable step size strategy.

2.3.1. The maximum voltage point (V_{mpp}) estimation

An ideal photovoltaic cell is a cell for which R_p is infinitely large. [22], [23]. The expression of the generated current is given by the following equation [23], [24]:

$$I = I_{ph} - I_o \left[\exp \left(\frac{V + R_s I}{n N_{sc} V_T} \right) - 1 \right] \quad (3)$$

Maximum power $P_{mpp} = I_{mpp} \times V_{mpp}$ is obtained by canceling the derivation of the power [25]:

$$\left(\frac{dP}{dI_{pv}} \right) = \frac{d(I_{pv} \times V_{pv})}{dI_{pv}} = 0 \quad (4)$$

which leads to,

$$\left(\frac{dV}{dI_{pv}} \right)_{mpp} = - \frac{V_{mpp}}{I_{mpp}} \quad (5)$$

The derivative of the Eq. (3) put into Eq. (5) gives:

$$\frac{V_{mpp}}{I_{mpp}} = -\frac{V_T}{(I_{sc} + I_o - I_{mpp})} \quad (6)$$

Taking into account Eq. (2), V_{mpp} can be found as

$$V_{mpp} = \frac{I_{mpp} \times V_T}{\left(1 - \frac{1}{K_i}\right) I_{mpp} - I_o} \quad (7)$$

The I_{mpp} is deducted from Eq. (5) and Eq. (7):

$$I_{mpp} = K_i I_o \left[\exp\left(\frac{V_{oc}}{nN_{sc}V_T}\right) - 1 \right] \quad (8)$$

The maximum voltage of PV cell can be calculated from Eq. (5) and Eq. (8):

$$V_{mpp} = \frac{V_T \left[\exp\left(\frac{V_{oc}}{V_T}\right) - 1 \right]}{\left(1 - 1/K_i\right) \exp(V_{oc}/V_T) - 1} \quad (9)$$

2.3.2. The maximum current point (I_{mpp}) estimation

By supposing that I_{ph} equals to I_{sc} in Eq. (3), the exponential factor being very significant, factor "-1" can be overlooked. Eq. (3) can be reduced as:

$$I = I_{sc} - I_o \left[\exp\left(\frac{V + R_s I}{nN_{sc}V_T}\right) \right] \quad (10)$$

Using Eq. (10) to obtain I_o , considering that the PV panel is at the open-circuit current point, which means that I is equal to 0. The relation I_o is given by the relation below:

$$I_o = I_{sc} \left[\exp\left(-\frac{V_{oc}}{nN_{sc}V_T}\right) \right] \quad (11)$$

Putting I_o from the above Eq. (10), lead to the following equation:

$$I = I_{sc} \left[1 - \exp\left(\frac{V - V_{oc} + R_s I}{nN_{sc}V_T}\right) \right] \quad (12)$$

Using Eq. (10) to solve V_T , the PV panel is assumed to be at the maximum power point, i.e. $V=V_{mpp}$ and $I=I_{mpp}$, so the previous equation can be re-ordered as:

$$V_T = \frac{V_{mpp} - V_{oc} + R_s I_{mpp}}{nN_{sc} \ln\left(1 - \frac{I_{mpp}}{I_{sc}}\right)} \quad (13)$$

Inserting the values of V_T from the Eq. (12) lead to:

$$I = I_{sc} \left[1 - \exp\left(\frac{(V - V_{oc} + R_s I) \times \ln\left(1 - \frac{I_{mpp}}{I_{sc}}\right)}{V_{mpp} - V_{oc} + R_s I_{mpp}}\right) \right] \quad (14)$$

The relation of I_{mpp} have been derived by putting Eq. (1) and Eq. (2) into Eq (14).

$$I_{mpp} = \frac{K_i I}{1 - \exp\left(\frac{(V - V_{oc} + R_s I) \times \ln(1 - K_i)}{V_{oc}(K_v - 1) + \frac{I_{sc}}{K_i} R_s}\right)} \quad (15)$$

2.3.3. D_{mpp} estimation

In PV systems, DC-DC converter (boost, buck, etc...) is used between PV panel and the load. For that MPPT engineered utilizes DC-DC converter to vary R_{out} . The expression between input voltage (V_{in}) and output voltage (V_{out}) of a boost converter illustrated in Fig. 1 can be expressed by:

$$V_{int} = \frac{1}{1-D} V_{out} \quad (16)$$

where, D is duty cycle. If we have 100% performance, we can assume $P_{out} = P_{in}$, therefore:

$$I_{out} V_{out} = I_{in} V_{int} \Rightarrow \frac{(V_{out})^2}{R_{out}} = \frac{(V_{int})^2}{R_{in}} \quad (17)$$

By using Eq. (16) and Eq. (17), it can be written as :

$$R_{in} = \frac{1}{(1-D)^2} R_{out} \quad (18)$$

The relation of the DC-DC boost converter can be rewritten by two equations in two different points at non-MPP by Eq. (19) and at MPP by Eq. (20).

$$R_{in} = \frac{1}{(1-D)^2} R_{out} \Rightarrow R_{in} = \frac{1}{(1-D)^2} \frac{V}{I} \quad (19)$$

$$R_{in} = \frac{1}{(1-D)^2} R_{out} \Rightarrow R_{in} = \frac{1}{(1-D_{mpp})^2} \frac{V_{mpp}}{I_{mpp}} \quad (20)$$

by equalizing the Eq. (19) and Eq. (20), then adding the expressions of V_{mpp} from Eq. (9) and I_{mpp} from Eq. (15) in the latter, the result lead to the relation of new duty cycle D_{mpp} below:

$$D_{mpp} = 1 - \left((1-D) \times \sqrt{\frac{V_T \left[\exp\left(\frac{V_{oc}}{V_T}\right) - 1 \right] \times \left[1 - \exp\left(\frac{(V - V_{oc} + R_s I) \times \ln(1 - K_i)}{V_{oc}(K_v - 1) + \frac{I_{sc}}{K_i} R_s}\right) \right]}{K_i \times V \times \left[\left(1 - 1/K_i\right) \exp(V_{oc}/V_T) - 1 \right]}} \right) \quad (21)$$

2.3.4. Comprehensive architecture of the MPPT method

It has three fundamental parameters: I_{mpp} , V_{mpp} and D_{mpp} which represent the maximum current, the maximum voltage and the duty cycle respectively. The relations are respectively given by Eq. (9), Eq. (15), and Eq. (21). The proposed technique is shown in Fig. 3.

This algorithm consists of three steps. The algorithm starts with a measurement of the short-circuit current and

then uses the FSCC algorithm (blue loop). Since the algorithm enters the red loop while the PV generator is running at MPP and is responsible for setting the PV generator P_{pv} near the MPP neighborhood by the D_{mpp} relationship expressed in Eq (21). Finally, in the green loop, the algorithm imposes the V_{mpp} and I_{mpp} criteria which are calculated from Eqs (9) and (15) respectively, which are described in the previous section. The proposed method remains in this loop until the limits are exceeded. If the limits are exceeded, the algorithm returns to the blue loop and the dynamic operation is restarted.

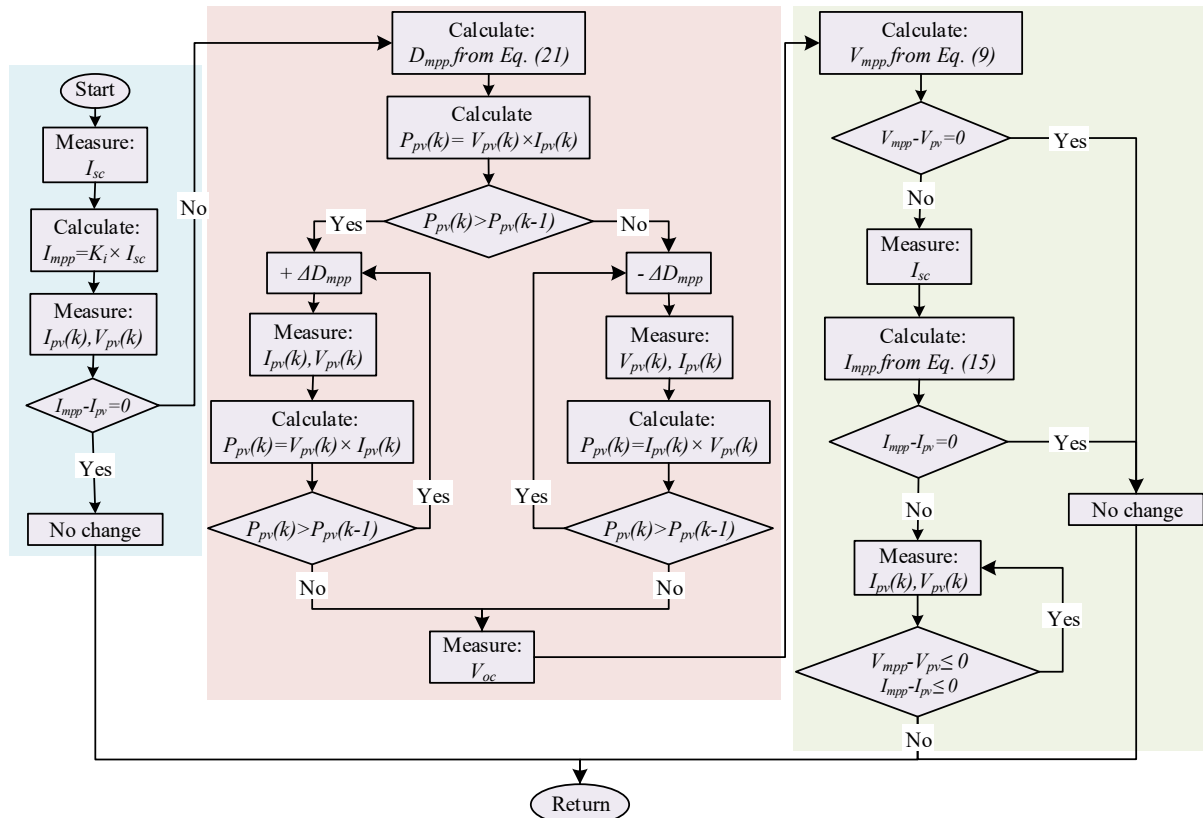


Fig. 3. The State flowchart of the enhanced algorithm.

3. Experimental tests and results

In this section, a comparison of the experimental results of the hill climbing and the enhanced MPPT algorithm is presented. In order to compare their algorithms, some parameters to evaluate their performance are described. Subsequently, a comprehensive description of the different elements of the experimental test bench used in this work is proposed. Finally, the results of experiments in different weather conditions are discussed.

3.1. Parameters for the evaluation of MPPT algorithm

Some well-known parameters can evaluate the effectiveness of an MPPT algorithm and assess its performance, like the tracking efficiency given by Eq. (22), the ripple rate of Eq. (23), the average power given by Eq. (24), the response time and the implementation complexity. The above criteria are appropriate for simulation tests [3]-[5],

[22], [25] but are less relevant in outside experiments which are subject to changing and random conditions. Nevertheless, simulations will never allow the fully characterization of a PV panel and its power tracking strategy [5], [10], [25].

In this paper, the MPPT methods described in Section II are tested and assessed using real conditions of temperature and irradiance. The different measurements (voltage, current and power) are accessed by the ControlDesk software to calculate the tracking efficiency, ripple rate, average power, and response time. These data are used to verify the performance of different MPPT methods.

The tracking efficiency (η) is an important parameter in the MPPT algorithm. This value is calculated as follows [7], [10]:

$$\eta = \frac{\int_0^t P_{mpt}(t) dt}{\int_0^t P_{max}(t) dt} \times 100 \quad (22)$$

The ripple rate of the power (τ_o) is the ratio between the efficiency value and the average value of the ripple [8], [10].

$$\tau_o = \frac{P_{pv_ond}}{\bar{P}_{pv}} \quad (23)$$

where P_{pv_ond} is the effective power of the PV panel.

The average power (P_m) is the PV output power under the control of MPPT over some period of time T . It is calculated as follows [8], [10]:

$$P_m = \frac{1}{T} \int_0^T P_{mppt}(t) dt \quad (24)$$

The response time (τ_r) corresponds to the time needed to reach the new MPP value.

3.2. Implementation aspects

The experimental evaluation of the MPPT algorithms performance is verified by using the test bench which is illustrated in Fig. 4. This bench was designed and implemented at the IRIMAS Laboratory, located in IUT of Mulhouse of the University of Haute Alsace in France. The test bench consists of the following elements:

A photovoltaic solar panel Solarex Solex FSM 145W-24 placed outside the building, following the south-east orientation (whose characteristics are given in Table 1). Two sensors TSL2591 and DHT11 are used to record irradiance and temperature respectively. These data are stored in an SD card via the Arduino Ethernet module with a sampling period of one second (refers to Fig. 4a).

As shown in Fig. 4b, the current sensor Probe Model PR20 and voltage sensor Model ST 1000-II are used to acquire the current and voltage output of the solar panel. Both of these data are used as input variables for the MPPT

controller to produce a PWM signal. The Semikron Semiteach - IGBT DC-DC converter, engineered to operate in continuous inductive current mode (whose specifications of which are given in Table 2), is directly linked to the PWM controller, which receives and amplifies the signal of the Slave port I/O PWM of the dSPACE1104 control Board. This signal will be utilized to control the IGBT power of the DC-DC boost converter, which in turn will shift the operating power to the MPP and achieve maximum operating performance. The load linked to the output of the DC-DC boost converter is a load of 120 Ω , chosen to facilitate the study. A digital oscilloscope WavaJet LeCroy visualizes at all times the signals (voltage, current, PWM signal and power).

The DS1104 Control Board is linked to a computer containing the experimental ControlDesk software and Matlab/Simulink software. The studied MPPT algorithms are schematically implemented in Matlab/Simulink via blocks from the Simulink libraries. Then, exploiting the features of the real-time interface toolbox (i.e., the RTI data block with a simplest frequency of 10 KHz) available in the Simulink libraries. The implemented MPPT algorithms are interfaced with the hardware.

The ControlDesk software allows managing to process hosted on the control board. It has been used as a signal acquisition system, which is intended to

- acquire and store the measured signals,
- give access to the display of the various curves,
- facilitate real-time analysis of the MPPT method performance in controlling the PV system.

The hardware platform is permanently linked to the desktop computer for interactive control, status monitoring and code download.

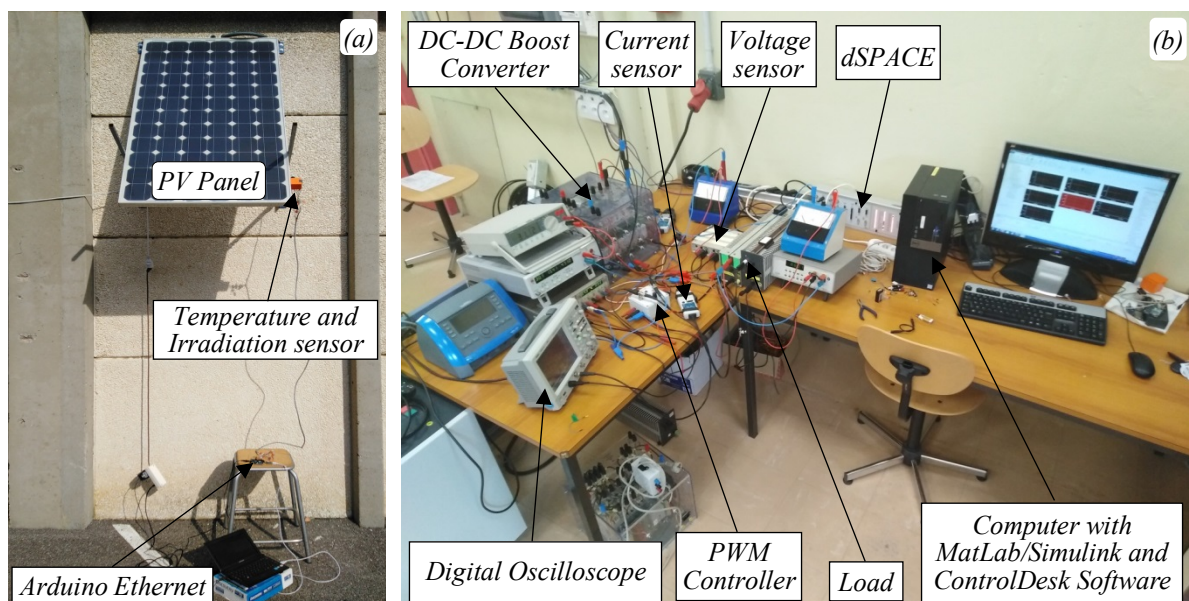


Fig. 4. The experimental test bench setup

Table 1: Electrical parameters of the Solarex Solex FSM 145W-24.

| Parameters | Values | Symbols |
|---|---------|-----------|
| Maximum power (W) | 145 | P_{mpp} |
| Temperature coefficient of I_{sc} (A/K) | 0.0065 | k_{sc} |
| Maximum Current (A) | 4.2 | I_{mpp} |
| Maximum voltage (V) | 34.4 | V_{mpp} |
| Parallel cell | 1 | N_p |
| Temperature coefficient of V_{oc} (V/K) | -0.3609 | k_{oc} |
| Open-circuit Voltage (V) | 43.5 | V_{oc} |
| Series cells | 72 | N_{sc} |
| Short-circuit current (A) | 4.7 | I_{sc} |

Table 2: Parameters of DC-DC boost converter

| Parameters | Values | Symbols |
|---------------------------------------|--------|-----------|
| Rated input current (A) | 30 | I_{in} |
| Boost inductor (mH) | 1.0 | L |
| Input filter capacitor (μF) | 90 | C_{in} |
| Output filter capacitor (μF) | 47 | C_{out} |
| Rated output current (A) | 30 | I_{out} |
| Rated output voltage (V) | 400 | V_{out} |
| Maximum Switching frequency (KHz) | 50 | f |

3.3. Experimental results and discussion

The experimental test bench in Fig. 4 is used to obtain the acquisition of measured data to validate the proposed method. The experiment is performed under an average irradiation of 876 W/m^2 and at an average ambient temperature of 31°C recorded by their respective sensors on

Thursday, September 20, 2018, local time in France. During the experiment, the experimental results of the start and equilibrium conditions were recorded using the control panel map. In addition, these data were utilized to assess and compare the performance of each MPPT algorithm in monitoring the true maximum power point (MPP).

It is clear from Fig. 5 that the true MPP is 100 W . The experimental starting waveforms for the current, voltage and PV output power extracted by hill climbing MPPT method, and the proposed method are presented in Fig. 5 (a) and (b) respectively. From the waveforms illustrated in Fig. 5, it can be seen that the current and voltage starting points are around 0.2 A and 37 V respectively. In addition, the PV output power and current increase during the start-up phase while the voltage decreases. In this experiment, the algorithms studied all converge towards the neighborhood of the exact PMP (100 W) But with various response times and oscillation rates (see Table 4). In steady state, the extracted power is measured and saved by the data acquisition control desk with a sampling period of 1 ms for each MPPT algorithm.

Fig. 6 shows the duty cycle variation for both controllers. With the proposed method, the optimized duty cycle is achieved more quickly and has less steady-state oscillations.

In order to elucidate the degradation in steady-state effectiveness, the average power output, power ripples and efficiency of the experiment are collected and evaluated in Table 4. On the basis of Table 3 and Fig. 7, it is clear that hill climbing method has been impacted in terms of effectiveness, resulting in substantial losses in the power produced. The proposed method's performance was not significantly affected, and consequently, the power ripples in the proximity of the MPP were negligible. An efficiency of 98.45% was also obtained.

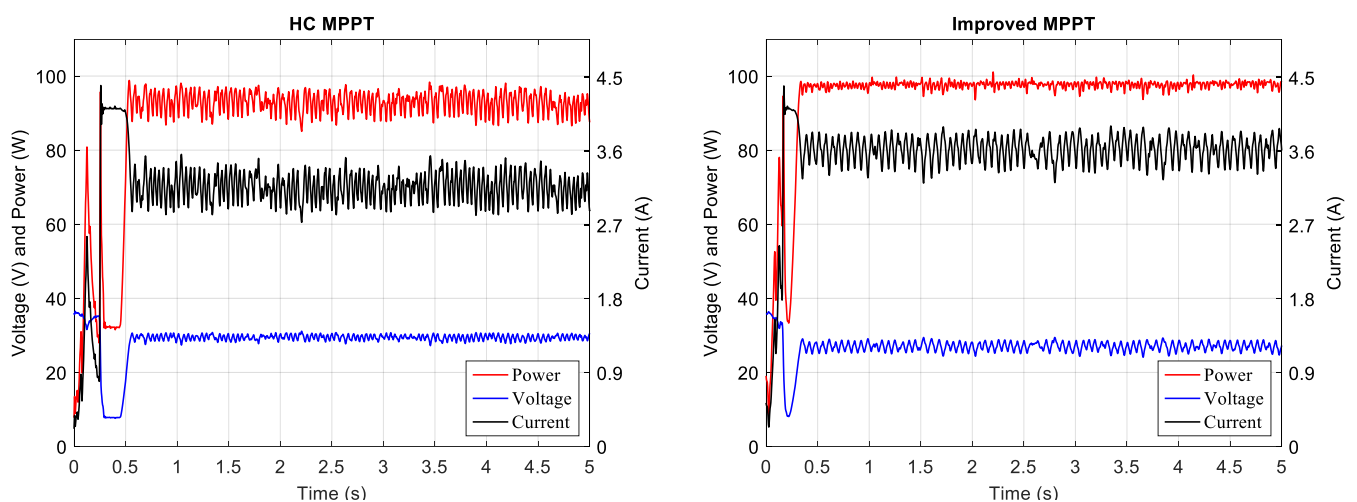


Fig. 5. Experimental PV curves of voltage, power and current for different methods for the test

Table 3: MPPT comparison

| | Hill Climbing MPPT Algorithm | Improved MPPT Algorithm |
|----------------|---------------------------------|----------------------------|
| PV power (W) | 90 | 98.28 |
| PV voltage (V) | 30 | 27.3 |
| PV current (A) | 3 | 3.6 |

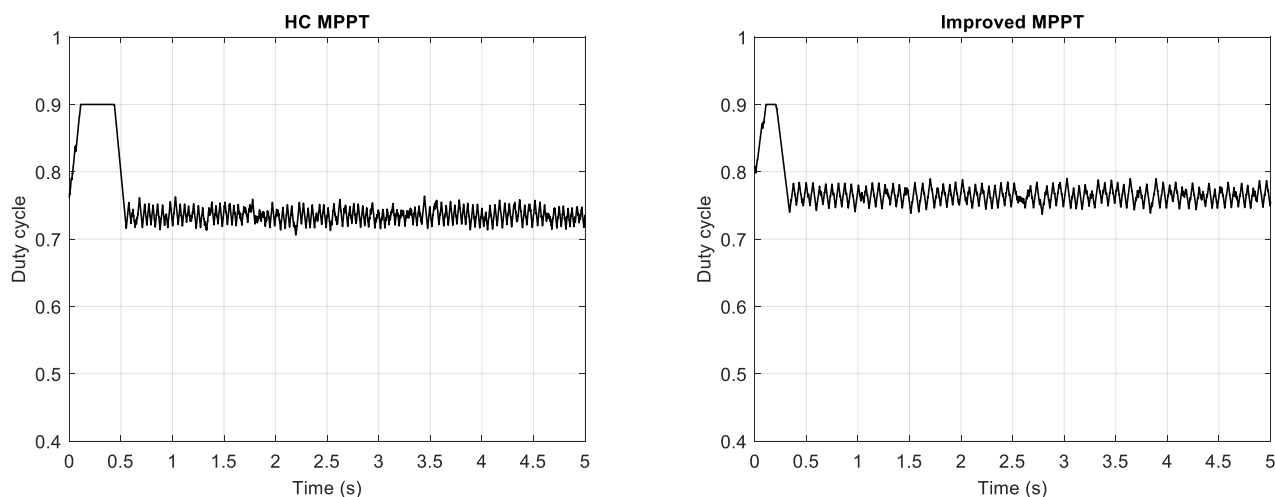


Fig. 6. Comparison of duty cycle for different methods for the test

Table 4 presents the results obtained with the MPPT algorithms, that is to say the conventional hill climbing approach and the proposed approach. Eq. (22), Eq. (23) and Eq. (24) were used respectively to calculate different parameters such as the tracking efficiency, the ripple rate and the average power.

From Fig. 7, Table 3 and Table 4, it is clearly observed that the proposed method has insignificant power ripples and

very good reliability in monitoring the MPP. As a result, the energy losses are very low, as the monitoring efficiency obtained by the proposed method is 98.45%. The steady-state performance of hill climbing MPPT algorithm has considerable power undulations (0.9 W), which results in lower efficiency in MPP monitoring (92.75%) and considerable energy losses compared to the proposed method.

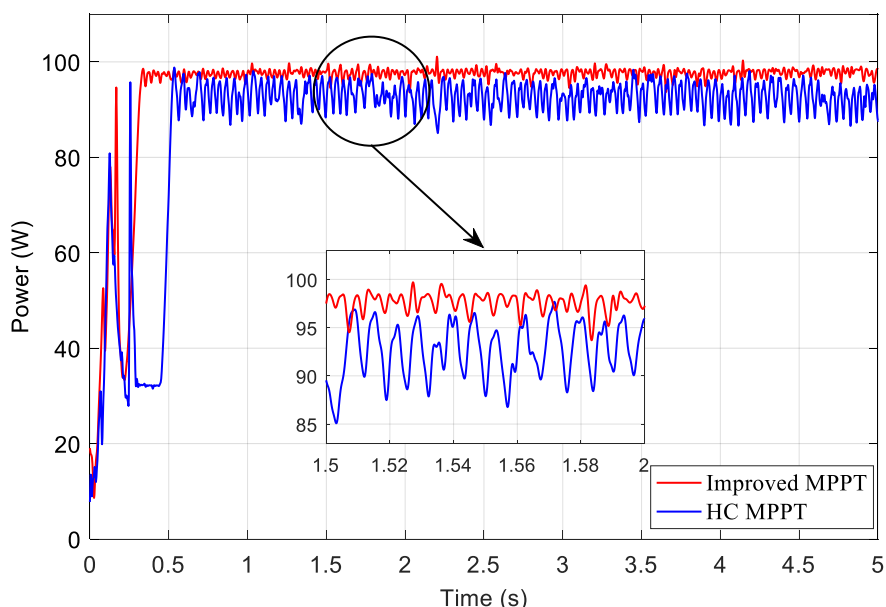


Fig. 7. Experimental curves of power for different methods

Table 4. Performance and comparison of the different MPPT methods for experiment

| Temperature, Irradiance | Parameters | Hill Climbing MPPT Algorithm | Improved MPPT Algorithm |
|---------------------------------------|------------------------------------|------------------------------|-------------------------|
| T= 31 °C, G = 876 W/m ² | Efficiency η (%) | 92.75 | 98.45 |
| | Ripple rate of the power t_o (W) | 2.5 | 0.5 |
| | Average power P_m (W) | 93 | 98 |
| | Response time τ_r (s) | 0.6 | 0.25 |
| | The used sensors | Voltage, Current | Voltage, Current |
| | Initial setting parameters | 2 parameters | 2 parameters |
| | Implementation complexity | Low | Medium |

4. Conclusion

The energy efficiency of the photovoltaic system depends on good performance with maximum power point tracking (MPPT) algorithms to extract the maximum power. An enhanced MPPT algorithm has been proposed in this document for this purpose. The proposed MPPT algorithm has been developed to solve the problems of the conventional MPPT hill climbing method. Indeed, the proposed algorithm is based on the estimation of the boost converter duty cycle associated with the conventional hill climbing algorithm. These techniques have been experimented and tested under real weather conditions. The experimental implementation has been designed with DS1104 control board, allows a comparison of the performance of the enhanced algorithm and the conventional hill climbing by calculating their tracking efficiency, ripple rate, average power and response time. In changing conditions, the proposed algorithm offers greater a precision and a better efficiency than the conventional hill climbing MPPT method.

Acknowledgement

Claude Bertin NZOUNDJA FAPI would like to personally express his gratitude to the Pierre-et-Jeanne Spiegel Foundation for its financial support.

Conflict of Interest

The authors declares that there is no conflict of interest.

References

- [1] A. Belkaid, I. Colak and K. Kayisli, "A Comprehensive study of different photovoltaic peak power tracking methods", *6th International Conference on Renewable Energy Research and Applications (ICRERA)*, San Diego, USA, pp. 1073-1079, 5-8 Nov. 2017.
- [2] C. B. Nzoundja Fapi, P. Wira and M. Kamta, "A Fuzzy Logic MPPT Algorithm with a PI Controller for a Standalone PV System under Variable Weather and Load Conditions", *IEEE International Conference on Applied Smart Systems (ICASS)*, Medea, Algeria, pp. 1-6, 24-25 Nov. 2018.
- [3] F. L. Tofoli, D. de C. Pereira, and W. J. de Paula, "Comparative Study of Maximum Power Point Tracking Techniques for Photovoltaic Systems", *International Journal of Photoenergy - Hindawi*, vol. 2015, pp. 1-10, Jan. 2015.
- [4] A. Gupta, Y. K. Chauhan and R. K. Pachauri, "A comparative investigation of maximum power point tracking methods for solar PV system", *Solar Energy*, vol. 136, pp. 236-25, 2016.
- [5] M. Danandeh and S. M. Mousavi, "Comparative and comprehensive review of maximum power point tracking methods for PV cells", *Renewable and Sustainable Energy Reviews*, vol. 82, pp. 2743-2767, 2018.
- [6] V. R. Kolluru, R. K. Patjoshi and R. Panigrahi, "A Comprehensive Review on Maximum Power Tracking of a Photovoltaic System Under Partial Shading Conditions", *International Journal of Renewable Energy Research (IJRER)*, vol. 9, no. 1, pp. 175-185, March, 2019.
- [7] A. Belkaid, I. Colak and K. Kayisli, "Implementation of a modified P&O-MPPT algorithm adapted for varying solar radiation conditions", *Electrical Engineering - Springer*, vol. 99, no. 3, pp 839-846, 2017.
- [8] H. A. Sher, A. F. Murtaza, A. Noman, K. E. Addoweesh, K. Al-Haddad, and M. Chiaberge, "A New Sensorless Hybrid MPPT Algorithm Based on Fractional Short-Circuit Current Measurement and P&O MPPT", *IEEE Transactions on Sustainable Energy*, vol. 6, no. 4, pp. 1426-1434, 2015.
- [9] M. M. Shebani, T. Iqbal, and J. E. Quaicoe, "Comparing Bisection Numerical Algorithm with Fractional Short Circuit Current and Open Circuit Voltage Methods for MPPT Photovoltaic Systems", *IEEE Electrical Power and Energy Conference (EPEC)*, Ottawa, Canada, 12-14 Oct., 2016.
- [10] R. Boukenoui, M. Ghanes, J.-P. Barbot, R. Bradai, A. Mellit and H. Salhi, "Experimental assessment of Maximum Power Point Tracking methods for photovoltaic systems", *Energy*, vol. 132, pp. 324-340, 2017.
- [11] W. Zhu, L. Shang, P. Li and H. Guo, "Modified hill climbing MPPT algorithm with reduced steady-state oscillation and improved tracking efficiency", *IET Journals, the Journal of Engineering*, vol. 2018, Iss. 17,

- pp. 1878-1883, 2018.
- [12] B. N. Alajmi, K. H. Ahmed, S. J. Finney, and B. W. Williams, "Fuzzy-Logic-Control Approach of a Modified Hill-Climbing Method for Maximum Power Point in Microgrid Standalone Photovoltaic System", *IEEE Transactions on Power Electronics*, vol. 26, no. 4, pp. 1022-1030, 2011.
- [13] D. Haji and N. Genc, "Fuzzy and P&O Based MPPT Controllers under Different Conditions", *7th International Conference on Renewable Energy Research and Applications (ICRERA)*, Paris, France, pp. 649-655, 14-17 Oct. 2018.
- [14] N. A. Ahmad and R. Dhaouadi, "Efficiency optimization of a DSP-based standalone PV system using fuzzy logic and dual-MPPT control", *IEEE Transactions on Industrial Informatics*, vol. 8, no. 3, pp. 573-584, 2012.
- [15] K. Amara, A. Fekik, E. B. Bourennane, T. Bakir and A. Malek, "Improved Performance of a PV Solar Panel with Adaptive Neuro Fuzzy Inference System ANFIS based MPPT", *7th International Conference on Renewable Energy Research and Applications (ICRERA)*, Paris, France, pp. 1098-1101, 14-17 Oct. 2018.
- [16] J. Ahmed and Z. Salam, "An improved perturb and observe (P&O) maximum power point tracking (MPPT) algorithm for higher efficiency", *Applied Energy*, vol. 150, pp. 97-108, 2015.
- [17] A. F. Murtaza, M. Chiaberge, F. Spertino, U. T. Shami, D. Boero and M. D. Giuseppe, "MPPT technique based on improved evaluation of photovoltaic parameters for uniformly irradiated photovoltaic array", *Electric Power Systems Research*, vol. 145, pp. 248-263, 2017.
- [18] T. Radjai, L. Rahmani, S. Mekhilef and J. P. Gaubert, "Implementation of a modified incremental conductance MPPT algorithm with direct control based on a fuzzy duty cycle change estimator using dSPACE", *Solar Energy*, vol. 110, pp. 325-337, 2014.
- [19] R. Boukenoui, R. Bradai, A. Mellit, M. Ghanes and H. Salhi, "Comparative Analysis of P&O, Modified Hill Climbing-FLC, and Adaptive P&O-FLC MPPTs for Microgrid Standalone PV System", *4th International Conference on Renewable Energy Research and Applications (ICRERA)*, Palermo, Italy, pp. 1095-1099, 22-25 Nov. 2015.
- [20] A. Murtaza, M. Chiaberge, M. D. Giuseppe and D. Boero, "A duty cycle optimization based hybrid maximum power point tracking technique for photovoltaic systems", *Electrical Power and Energy Systems*, vol. 59, pp. 141-154, 2014.
- [21] X. Li, H. Wen and Y. Hu, "Evaluation of Different Maximum Power Point Tracking (MPPT) Techniques based on Practical", *5th International Conference on Renewable Energy Research and Applications (ICRERA)*, Birmingham, UK, pp. 696-701, 20-23 Nov. 2016.
- [22] R. J. Mukti and A. Islam, "Modeling and Performance Analysis of PV Module with Maximum Power Point Tracking in Matlab/Simulink", *Applied Solar Energy - Springer*, vol. 51, no. 4, pp. 245-252, 2015.
- [23] E. M. G. Rodrigues, R. Godina, M. Marzband and E. Pouresmaeil, "Simulation and Comparison of Mathematical Models of PV Cells with Growing Levels of Complexity", *Energies (MDPI)*, vol. 11, no. 2902, pp. 2-21, 2018.
- [24] I. E. Batzelis, "Simple PV performance equations theoretically well founded on the single-diode model," *IEEE Journal of Photovoltaics*, vol. 7, no. 5, pp. 1400-1409, 2017.
- [25] K. Kajiwarra, H. Tomura, N. Matsui and F. Kurokawa "Performance-Improved Maximum Power Point Tracking Control for PV System", *7th International Conference on Renewable Energy Research and Applications (ICRERA)*, Paris, France, pp. 1153-1156, 14-17 Oct. 2018.